Paper C-2 Chemical and Biochemical Engineering Quarterly

by Nita Aryanti

Submission date: 13-Jun-2020 01:46PM (UTC+0700)
Submission ID: 1342996479
File name: Artikel_untuk_TURNITIN_Cabeq_2018.pdf (4.23M)
Word count: 4400
Character count: 22571

Ultrafiltration Membrane for Degumming of Crude Palm Oil-Isopropanol Mixture

N. Aryanti,[a,b,*] D. Hesti Wardhani,[a] and A. Nafiunisa[a]

doi: 10.15255/CABEQ.2017.1244

Original scientific paper
Received: October 24, 2017
Accepted: August 1, 2018

Keywords:
crude palm oil, ultrafiltration, degumming

Introduction

Crude vegetable oil is a raw material used in the production of edible vegetable oil. Some examples of crude vegetable oils include crude palm oil (CPO), crude soybean oil, crude corn oil, crude coconut oil, crude sunflower oil, and crude castor oil[1]. Indonesia is one of the largest producers of CPO, followed by Malaysia, Thailand, Colombia, and Nigeria. Compared to other oilseed crops, palm oil produces more oil products[2]. Compared to other vegetable oils, it is preferable in many applications as it is substantially cost-effective[3]. CPO is widely used in various food and industrial products' manufacturing processes, such as ice cream, frying oils, shortening, cosmetics, toothpastes, and biodiesel[4]. CPO is extracted from the ripe mesocarp of the fruit of oil palm trees (*Elaeis guineensis*) through various methods, such as mechanical pressing followed by solid–liquid extraction[2].

The crude oil extracted from palm oil fruits is also rich in palmitic acid, β-carotene, and vitamin E, along with some undesirable compounds, such as phospholipids, free fatty acids (FFA), pigments, and proteins[5–6]. CPO is composed of a vast number of triglycerides (TAGs) and 6 % diglycerides (DAGs) that naturally consist of FFA[7]. Industrial regulations expect that high-quality oil must contain more than 95 % neutral TAGs and 0.5 % or less FFA; for some reason, the limit also decreases to less than 0.1 %[2,8].

Complex refining processes including degumming, neutralization, bleaching, and deodorization are performed to meet the desired requirement. The first step in the refining process is degumming, the function of which is to remove phospholipids and mucilaginous gums. Conventional degumming methods using water and acids possess numerous drawbacks due to the high energy consumption, oil loss, loss of nutrients, and requirement for large water quantities[9–10]. The membrane-based filtration process is a promising method for refining palm oil. Membrane filtration provides low energy consumption, without the addition of chemicals and with almost no loss of natural oil[11–12]. Previous studies on CPO refining using membrane filtration have been evaluated[3,13–17]. Arora *et al.*[3] evaluated the degumming of CPO and crude palm olein with a hexane solvent to remove phospholipids, Lovibond color value, carotenoids, major tocopherols and tocotrien-

ols, and major fatty acids. Ong *et al.*[13] studied ultrafiltration (UF) of CPO degumming for the removal of phospholipids, carotenes, Lovibond color, FFAs, and volatile matter. Lai *et al.*[14] performed research on the deacidification of a model fatty system of CPO using various solvents and nanofiltration. On the other hand, polyvinylidene fluoride (PVDF) has been modified with polyvinyl alcohol (PVA) crosslinked as a UF membrane in the deacidification of CPO[15]. Deacidification of CPO using an aqueous NaOH solution in a hollow fiber membrane contactor was carried out by Purwasasmita *et al.*[16] Furthermore, a hexane solvent combined with a UF membrane has been applied to remove phospholipids from residual palm oil fibers[17].

Similar molecular weights of TAGs and phospholipids (about 900 and 700 Da, respectively) can interfere with their separation process using membrane technology. Phospholipids tend to form reverse micelles in nonpolar media like hexane or crude oil because of their amphiphilic properties[18,19]. This unique feature of phospholipid micelles increases their average molecular weight from 700 Da to around 20 kDa or even more[12], which is significantly different from TAGs. As a result, the UF membrane is able to separate the micelles from the solvent–oil mixture, and the phospholipids are retained by the UF membrane[20]. However, the primary challenge in the use of membranes, especially UF, is the existence of a phenomenon called fouling. Fouling is an irreversible membrane change that is caused by specific physical and chemical interactions between the membrane and the various components present in the process flow. Membrane fouling is represented by a decrease in the permeate flux due to the effect of blocking on the surface as well as inside the membrane pores[21,22]. As it is essential to have a detailed investigation on fouling and there is no research investigating membrane fouling in the degumming of crude palm oil, this research is focused primarily on studying the flux decline as well as the fouling mechanism in the degumming of CPO by UF.

Fundamental studies on fouling mechanisms on UF membranes have been performed for coconut cream[23], organic compounds[24], whey models[25], and polyethylene glycol (PEG)[26]. In more detail, the fundamental studies focusing on the fouling mechanism in UF for oil degumming or separation of oil components are limited only for degumming corn oil[18–27], crude sunflower oil, and soybean oil[14]. This study placed emphasis on the fundamental and comprehensive analysis of the influence of oil solvents and micelles on fouling mechanism models. Specifically, this study addressed a novelty finding in the analysis of the fouling model and fouling mechanism in UF for degumming CPO.

Materials and methods

Materials

The main raw materials used in this experiment were CPO (Kalimantan, Indonesia) and isopropanol (Merck) as a solvent. The UF membrane was a laboratory-made polyethersulfone (PES) flat-sheet membrane. The PES material was Veradel PESU 3100P (Solvay, Singapore). The membrane was prepared via a non-solvent-induced phase separation method with PEG as the additive and N-methyl-2-pyrrolidone (NMP) as the solvent[28].

Membrane characterization

The membrane was characterized for its molecular weight cut-off (MWCO), contact angle, permeability, surface structure, and specific functional groups. The MWCO of the membrane represents the lowest molecular weight of solute (in Daltons), in which 90 % of the solute is rejected by the membrane. The MWCO value is evaluated to describe the pore size distribution and retention capabilities of membranes. In this work, solute rejection experiments were performed using PEG (from Sigma-Aldrich) as polymer solute with various molecular weights (MWs) of 2, 6, 12, 20 and 35 kDa. The PEG solution was prepared in 1 wt.% concentration and then filtrated in a dead-end filtration cell. The permeate samples were analyzed using a digital handheld refractometer (PAL-91S, ATAGO, Japan). Plots of MW versus solute rejection were created, and then the MW corresponding to 90 % rejection was estimated as MWCO of the membrane. The hydrophobic/hydrophilic character of the membrane was determined by measuring the water-membrane contact angle (θ). The water-membrane contact angle values of the prepared membrane were measured using water contact angle meter (RACE contact angle meter, Japan) using deionized water as a probe liquid.

Membrane permeability was evaluated by determining the membrane flux of distilled water or isopropanol in the membrane module at various operating pressures (1–3 bar). The fluxes were calculated according to the sample volume (V), the sampling time (t), and the membrane surface area (A). The volumetric permeate flow rate (Q) was calculated by

$$Q = \frac{V}{t} \tag{1}$$

Further, the flux (J) was determined by:

$$J = \frac{1}{A} \cdot Q \tag{2}$$

The membrane's surface and the cross-sectional structure were characterized using scanning electron microscopy (SEM, FEI Type Inspect-S50). The specific functional groups of the membrane were determined using FTIR Spectroscopy (Prestige-21, Shimadzu, Japan).

Evaluation of UF membrane performance for degumming of the CPO-isopropanol mixture

The UF performance was examined using laboratory-made cell filtration based on the total recycle model as illustrated in Fig. 1.

The cell filtration was equipped with a centrifugal pump (Kemflow, with nominal flow rate 1.0 LPM, maximum pump output of 7.58 bar, maximum inlet pressure of 4.14 bar) as the feed pump, gate valves, pressure gauge (JAKO, with maximum pressure of 10.34 bar) and a stainless steel ultrafiltration housing. The total recycle model involved returning the permeate and retentate flow back to the feed tank to maintain equivalent concentration during the process. All experimental runs were conducted at room temperature (29 ± 2 °C). Before starting the experiments, membranes were first compacted by filtering water through the membrane at a pressure of 1 bar for 60 min. For each run, a new circular membrane sheet with an effective area of 13.85 cm^2 was used.

A micellar solution was prepared by mixing CPO with isopropanol with ratios of CPO of 30 %, 40 %, 50 %, and 60 % weight of the solution. The filtration cell was operated at 1 bar for 120 min, and before returning it back to the feed tank, the permeate was collected every 5 min to determine the flux and concentration of phospholipids/fatty acids. The feed temperature was varied –30 °C, 35 °C, 40 °C, and 45 °C – in order to investigate the effect of temperature on UF performance. The feed tank was equipped with a temperature regulator and a magnetic stirrer for homogenization of oil micelles. Membrane performance was evaluated in terms of

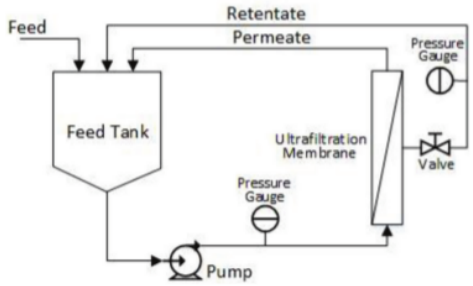

Fig. 1 – *Schematic of ultrafiltration cell with total recycle operation*

permeate flux and phospholipid/FFA rejection. Permeate fluxes (J) were determined by weighing the volume of the permeate collected at 5-min intervals for 120 min and calculated using

$$J = \frac{W}{A \cdot t} \tag{3}$$

Where W represents the total weight of the permeate, A is the membrane area, and t is the time interval.

Rejection of phospholipids and FFAs was determined on the basis of the concentration of phospholipids/FFAs in the feed (C_f) and in the permeate (C_p). Rejection is calculated according to

$$R = \frac{C_f - C_p}{C_f} \tag{4}$$

Characterization of CPO and permeate

The specific characteristics of CPO and permeate included the phospholipid and FFA content. Phospholipids were expressed as total phosphorus and analyzed according to the AOAC Ca 12–55 method. Determination of FFA was performed via the acid-base titration method[14].

Blocking mechanism

The blocking mechanism of CPO-isopropanol UF was studied according to Hermia's model. This model has been previously applied for the evaluation of the fouling mechanism of dye solution UF[28], konjac glucomannan separation[29], and UF of model dye wastewater[30]. Hermia's model describes the mechanism of membrane fouling on the basis of the blocking filtration law, consisting of complete pore blocking, standard pore blocking, and intermediate pore blocking and cake filtration. The blocking law filtration is expressed in terms of permeation time and filtration time, and was developed for dead-end filtration as shown in[31]:

$$\frac{d^2t}{dV^2} = k\left(\frac{dt}{dV}\right)^n \tag{5}$$

where t is the filtration time, V is the permeate volume, k is a constant, and n is a value illustrating the different fouling mechanisms.

The values of n are described as follows: complete blocking with $n = 2$, intermediate blocking with $n = 1$, standard blocking with $n = 1.5$, and cake layer formation with $n = 0$. In the complete blocking model, it is assumed that each solute participated in blocking the entrance of the membrane pores completely. In intermediate blocking, it is assumed that every solute stays on the previously deposited

solutes. Standard blocking considers the deposition of each solute on the internal pore wall. The cake layer formation occurs due to the accumulation of the solute on the membrane surface in a cake form[32]. Hermia's model was then linearized on the basis of the n value for each model by fitting equations (6) to (9) regarding the permeate flux versus time, as presented in the following.

For Complete Blocking ($n = 2$):

$$\ln J = \ln J_0 - k_c t \quad (6)$$

For Intermediate Blocking ($n = 1$):

$$\frac{1}{J} = \frac{1}{J_0} + k_i t \quad (7)$$

For Standard Blocking ($n = 1.5$):

$$\frac{1}{\sqrt{J}} = \frac{1}{\sqrt{J_0}} + k_s t \quad (8)$$

For Cake/Layer Formation ($n = 0$):

$$\frac{1}{J^2} = \frac{1}{J_0^2} + k_{cf} t \quad (9)$$

Here, k_c, k_i, k_s, and k_{cf} are constants for complete blocking, intermediate blocking, standard blocking, and cake layer formation, respectively.

Results and discussion

Membrane characteristics

Table 1 shows the characterization results of the synthesized membranes confirming PEG rejections, MWCO, contact angle, and permeabilities.

Details of the water and isopropanol flux profiles at various pressures for the UF membrane are presented in Fig. 2.

Table 1 – *Characteristics of the synthesized PES membrane*

Parameter	
Rejection of 2 kDa PEG (R)	9.83 %
Rejection of 6 kDa PEG (R)	13.11 %
Rejection of 12 kDa PEG (R)	68.85 %
Rejection of 20 kDa PEG (R)	88.52 %
Rejection of 35 kDa PEG (R)	96.72 %
MWCO	25 kDa
Contact angle (θ)	63.63°
Water permeability ($L_{h,w}$)	42.77 L m^{-2} h^{-1}
Isopropanol permeability ($L_{h,Isp}$)	63.58 L m^{-2} h^{-1}

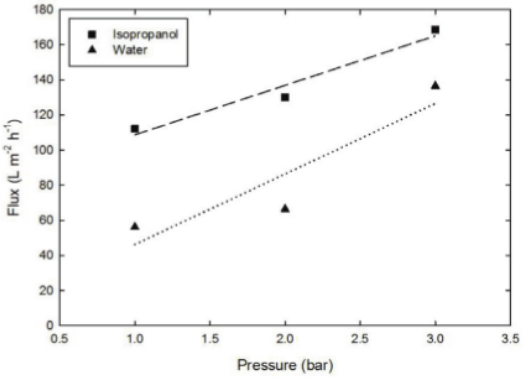

Fig. 2 – *Flux profile of isopropanol and water at pressure of 1–3 bar*

The figure shows an increase in water and isopropanol flux with the rise of pressure from 1 to 3 bar. According to the linearization regression ($y = mx$) of water and isopropanol flux in the figure, it was found that the water permeability and isopropanol permeability were 42.77 L m^{-2} h^{-1} and 63.58 L m^{-2} h^{-1}, respectively. This is surprising, since water is predicted to have permeability higher than that of ethanol which is why water is the most polar solvent. This result is in contrast with de Melo *et al.*[33], confirming that lower solvent polarity results in a decrease in permeation. In addition, the prepared PES membrane had the characteristics of hydrophilic membranes represented by the contact angle value as listed in Table 1, especially because of the addition of polyvinylpyrrolidone (PVP) and PEG[34]. With the hydrophilic characteristic of the PES membrane, water permeation is expected to be higher than that of isopropanol. Solvent characteristics, such as viscosity, surface tension, and polarity, as well as the molar volume of the solvent, have an effect on the transport of the solvent by the membrane[35–36]. According to the physicochemical characteristics of the solvent (viscosity and interfacial tension), the isopropanol flux should be below the water flux. However, this phenomenon was not observed in this research, presumably because there wasa specific interaction between the membrane and the solvent. A similar result was observed by Araki *et al.*[37] The high permeability of isopropanol indicates that the conditioning process (immersing in isopropanol) created a less hydrophilic PES membrane. The alteration of the hydrophobic characteristic is caused by the transformation of the hydrophilic and hydrophobic sites of the membrane, resulting in the higher permeability of isopropanol. Water permeation is correlated to the hydrophilic characteristic (hydrogen bond formation) of the membrane. When an alcohol such as isopropanol is permeated, the hydrogen bond formation becomes less, contributing to a low water flux.

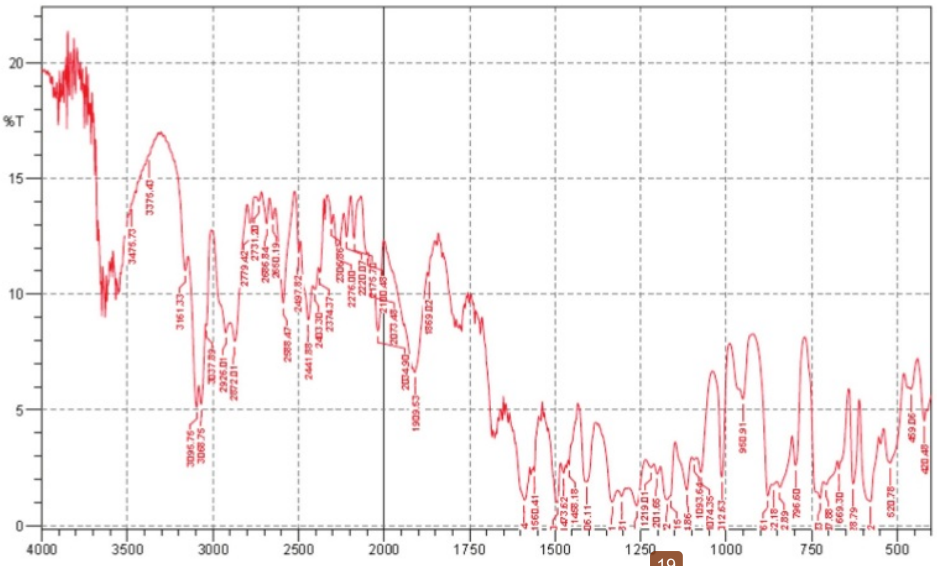

Fig. 3 – *FT-IR spectra of the membrane confirming specific functional groups*

Specific functional groups

Specific functional groups of the membrane are shown in Fig. 3.

According to the figure, characteristics of the PES membrane are determined by peaks at 1492.9 and 1589.3 cm^{-1}. Moreover, the peaks of 1161.15 and 1172.7 cm^{-1} show a symmetric stretching sulfur SO_2. In more detail, Table 2 lists other specific functional groups of the membrane.

Based on the table, the specific functional groups were matched with the chemical structure of main membrane materials. Beside the PES characteristic, the O-H bonding vibration, C-H asymmetric, C-C stretching in benzene ring and -C-O-C- bonding are representation of bonds in the polymer of PEG.

Permeate flux

The profile of the permeate flux showing flux versus time is presented in Fig. 4.

The figure shows that there is a flux decline during the filtration of the solvent and CPO mixtures. A significant flux fall-off was observed during the first 5 min of filtration, followed by a flux reduction deceleration rate, and then finally the flux became steady. A three-step behavior was also perceived by Penha *et al.*[38] during the filtration of maracuja oil/*n*-hexane mixture. The initial flux decline is caused by a phenomenon called polarization concentration, whereas the following flux reduction is a result of membrane fouling. Comparable performances were reported for oil/hexane mixture per-

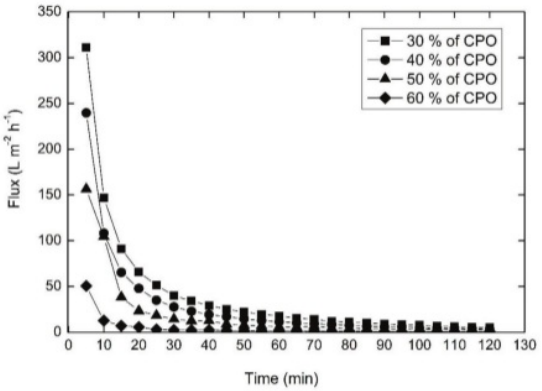

Fig. 4 – *Permeate flux profile in the UF of the CPO-isopropanol mixture at various concentrations of CPO (feed temperature: 29 °C, transmembrane pressure: 1 bar)*

Table 2 – *Specific functional groups as shown in FT-IR spectra*

Absorbance peaks (cm^{-1})	Specific functional groups
1473.41 and 1560.62	Aromatic compounds (C-C stretching)
1219.01 and 1261.4	Aromatic ether compounds
849.2 and 862.2	Para substituted benzene
1074.3, 1093.6 and 1114.8	-C-O-C- bonding
2872.01 and 2926.01	C-H asymmetric bonding
3375.43 and 3475.73	O-H alcohol bonding

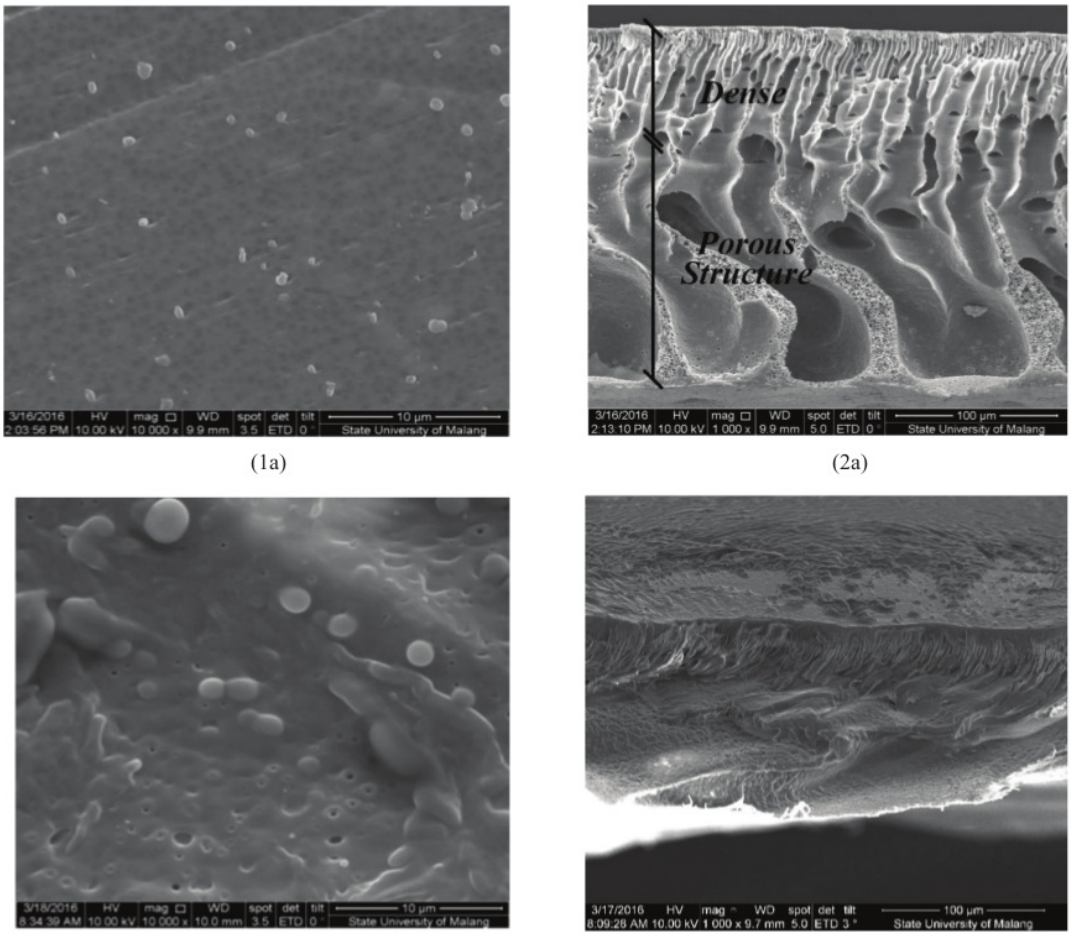

Fig. 5 – *SEM images at magnification of 10,000x: Clean membrane (1a- Surface), (2a- Cross-sectional structure) and fouled membrane after ultrafiltration of 30 % CPO-solvent mixture (1b-Surface), (2b-Cross-sectional structure)*

meation through the UF membrane using sunflower oil[39] as well as coconut oil, groundnut oil, mustard oil, sunflower oil, and rice bran oil [36-40]. In addition, it was reported that the flux reduction at the beginning of the sunflower oil–*n*-hexane filtration was type of concentration polarization phenomenon and gel layer formation on the membrane surface[39]. Moreover, the flux drop at the end of the filtration was due to the deposition of a gel on the membrane surface[38,41,42]. The deposited layer is formed because of the phospholipids retained on the membrane surface and pores plugging[14,43].

Fig. 4 also confirms that the increase in oil concentration leads to a higher reduction in flux. This decrease takes place due to an increase in oil concentration, resulting in the increase insolution viscosity. With the rise of viscosity, a smaller flux is obtained since the permeability is influenced by the viscosity[35]. In addition, a lower flux is obtained as a result of polarized/gel layer formation. When the oil concentration is higher, the layer becomes larger and generates larger resistance to the flux permeation[33,36,41]. As elucidated by Kim *et al.*[41], convective solute transport to the membrane produces a sharp gradient of concentration inside the boundary layer. Because of diffusion, solute back-transport into the bulk takes place, and a close-packed arrangement of the solute is formed. As a consequence, no more solute can be accommodated, and the mobility of solutes is restricted.

Scanning electron microscopy images of the fouled membrane, as displayed in Fig. 5, confirm that a foulant layer on the membrane's surface is present.

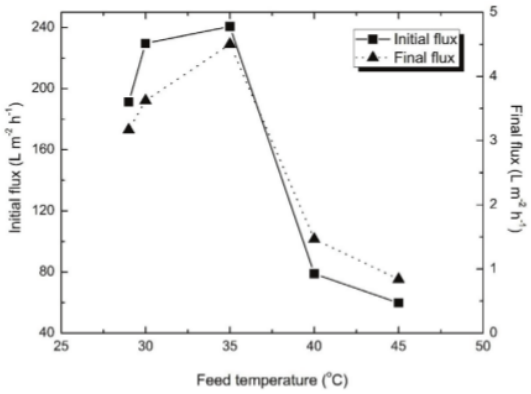

Fig. 6 – *Effect of feed temperature on the initial and final flux at a pressure of 1 bar and CPO concentration of 30 %*

Fig. 6 displays the effect of feed temperature on the initial and final permeate flux.

The figure suggests that the increase in the mixture temperature from 29 to 35 °C had an effect on the higher flux permeate. This was expected due to the decrease in viscosity or the increase in phospholipid diffusion on the membrane pores. However, a further temperature increase (from 40 to 45 °C) led to a decrease in flux, but the reduction in viscosity had no effect on the flux. This result is close to that of Kim *et al.*[41], confirming that the operating temperature of 40 °C was suitable for the degumming of soybean extract; above the temperature of 40 °C, the flux decreased. A decline in flux is predicted because of the fouling on the membrane surface as a result of solid denaturation or gelatinization, as well as insoluble salts precipitation at a high temperature[44].

Phospholipid and FFA rejection

Membrane selectivity is represented as rejection, indicating the membrane's ability to reject or remove a feed compound. Micelles are formed when phospholipids are dispersed in water. The mixture of phospholipids in a nonpolar solvent such as isopropanol formed reverse micelles having an average molecular weight of 20,000 Daltons (10–200 nm)[44]. Based on the pore size, UF rejects compounds having a molecular weight in the range of 300–500,000 Daltons. Hence, in the phospholipids-isopropanol system, phospholipids are expected to be retained in the retentate, and the permeate comprises the oil and isopropanol. In contrast to phospholipids, the MWs of FFAs and TAGs are similar. TAGs and FFAs have a molecular weight of 800 Da and 300 Da, respectively[9]. Compared to the UF pore size, the separation of FFAs is challenging due to the low selectivity, and it results in a low rejection value. Rejection of phospholipids and FFAs at various CPO concentrations is displayed in Table 3.

Table 3 – *Rejection of phospholipid and fatty acids at various CPO concentrations at a pressure of 1 bar and feed temperature of 30 °C*

CPO concentration	Phospholipid rejection (%)	Free fatty acid rejection (%)
30 %	>99.21	16.13
40 %	92.93	12.93
50 %	37.52	9.09

Table 4 – *Rejection of phospholipid and fatty acids at various feed temperatures at a pressure of 1 bar and CPO concentration of 30 %*

Temperature	Phospholipid rejection (%)	Free fatty acid rejection (%)
30 °C	>99.21	16.13
35 °C	86.60	7.17
40 °C	73.94	10.24

The table shows that rejection of phospholipids is significantly higher than that of fatty acids. This is noticeable since the molecular weight of micelle phospholipids is considerably greater than that of FFAs. The phospholipids' rejection is found to be greater than 99 % at a CPO concentration of 30 %, and slightly reduced to nearly 93 % with the increase in CPO concentration to 40 %. The reduction of phospholipid rejection becomes more obvious with the increase in CPO concentration to 50 %. In addition, a similar trend is shown when the feed temperature is raised. The rejection of both phospholipids and FFAs declines at higher temperatures from 30 °C to 40 °C, as presented in Table 4.

Blocking mechanism by Hermia's model

In this research, Hermia's model was applied in order to evaluate the blocking mechanism during UF of the CPO-isopropanol mixture at various feed CPO concentrations. The fouling mechanism represented by the blocking mechanism is identified by fitting the experimental data into Hermia's linearized equation (equations (4) to (7)). The fitting of experimental data to the four-type Hermia model is shown in Fig. 7, and the corresponding correlation coefficients (R^2) are listed in Table 5.

According to the table, two dominant blocking mechanisms are found: standard blocking and intermediate blocking. At low concentrations of CPO (30 % and 40 %), the blocking mechanism is dominated by standard blocking. In contrast, at higher concentrations of CPO (50 % and 60 %), the intermediate blocking is the dominant mechanism. Standard blocking assumes that each solute is deposited into the internal pore wall. In intermediate blocking,

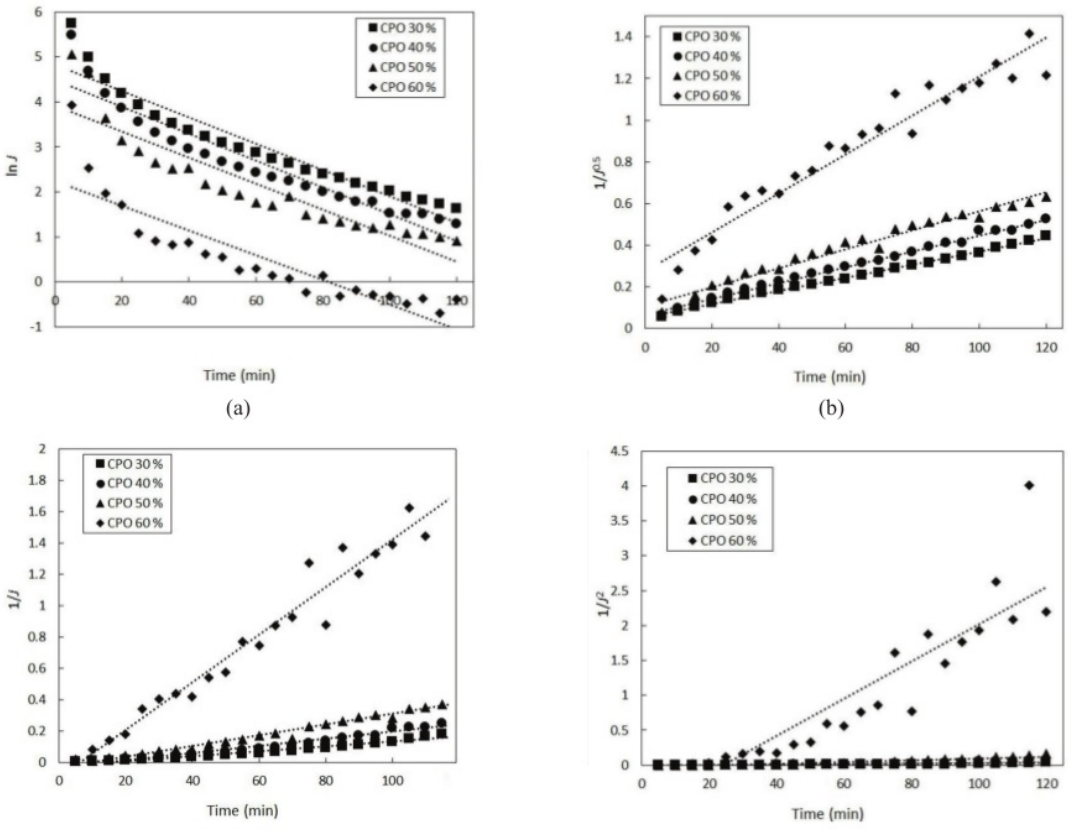

Fig. 7 – *Fitting of experimental data (feed temperature: 30 °C, pressure: 1 bar) to Hermia's model: (a) complete blocking, (b) standard blocking, (c) intermediate blocking, and (d) cake/gel layer formation*

Table 5 – *R^2 values of the blocking mechanism based on Hermia's model*

Feed concentration	R^2			
	Complete blocking	Intermediate blocking	Standard blocking	Cake/Gel formation
CPO 30 %	0.9186	0.9512	0.9971	0.7755
CPO 40 %	0.9022	0.9618	0.9953	0.8053
CPO 50 %	0.8354	0.9811	0.9737	0.8769
CPO 60 %	0.7797	0.9432	0.9394	0.8052

it is proposed that every solute remains on the previously deposited solutes.

The proposed standard blocking and intermediate blocking mechanisms in UF of CPO-isopropanol are illustrated in Fig. 8.

According to Fig. 8(a), the large particles that accumulated on the membrane surface and blocked the membrane pores were TAGs. The large particles that formed at a high concentration of CPO were first presumed to be phospholipid-isopropanol micelles because of their large size and potential to block the pores. However, this assumption is in contradiction with phospholipid rejection. If the large particles were an agglomeration of phospholipid micelles, then rejection at high CPO concentrations should be greater. Hence, it can be assumed that, at high concentrations of CPO, not all phospholipids generate micelles with isopropanol. This confirms why phospholipid rejection at high concentrations of CPO was lower. Hence, the larger particles that accumulated on the membrane surface were predicted to be other oil compounds such as TAGs.

In addition, Fig. 8(b) shows that, at low concentrations of CPO, the dominant fouling mechanism was standard blocking, representing small particles attached inside the membrane pore, and causing pore constriction (reduction in pore size). The compound that was possibly blocking the membrane pores was fatty acid, since fatty acids are smaller than phospholipid-isopropanol micelles. At

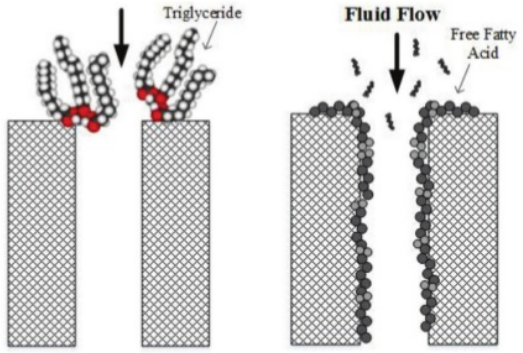

Fig. 8 – *Schematic illustration of (a) intermediate blocking and (b) standard blocking mechanisms in UF of the CPO-isopropanol mixture*

low concentrations of CPO, a sufficient amount of phospholipid-isopropanol micelles was formed, with pore constriction providing high rejection of phospholipids. On the other hand, small molecules, such as fatty acids, can enter the membrane pores.

Conclusions

Phospholipids separation and FFAs removal in CPO have been performed using a PES UF membrane. In general, lower fluxes were obtained with increase in CPO concentration. Raising the feed temperature from 30 °C to 40 °C resulted in a lower permeate flux, but further feed temperature increase to 45 °C decreased the permeate flux. The phospholipid rejection rate was in the range 93–99 %. However, the removal of fatty acids was unsuccessful. The decrease in flux due to membrane fouling was evaluated on the basis of Hermia's model, confirming that there were two dominant mechanisms observed: standard blocking and intermediate blocking.

ACKNOWLEDGEMENTS

Luh Astla Diva Savitri and Asih Mustika Sari were appreciated for their valuable research assistance. [illegible] acknowledges the Directorate of Research and Community Service, Ministry of Research and Higher Technology, the Republic of Indonesia for the financial support. The research was funded by the Fundamental Research Grant.

Paper C-1 Chemical and Biochemical Engineering Quarterly

ORIGINALITY REPORT

20%	%	20%	%
SIMILARITY INDEX	INTERNET SOURCES	PUBLICATIONS	STUDENT PAPERS

PRIMARY SOURCES

1	N Aryanti, D H Wardhani, Z S Maulana, D Roberto. "Evaluation of Ultrafiltration Performance for Phospholipid Separation", Journal of Physics: Conference Series, 2017 Publication	13%
2	Tutuk Djoko Kusworo, Qudratun, Dani Puji Utomo. "Performance evaluation of double stage process using nano hybrid PES/SiO 2 - PES membrane and PES/ZnO-PES membranes for oily waste water treatment to clean water", Journal of Environmental Chemical Engineering, 2017 Publication	2%
3	Nita Aryanti, Tutuk Djoko Kusworo, Wiharyanto Oktiawan, Dyah Hesti Wardhani. "Performance of Ultrafiltration–Ozone Combined System for Produced Water Treatment", Periodica Polytechnica Chemical Engineering, 2019 Publication	1%
4	Ana García, Silvia Álvarez, Francisco Riera, Ricardo Álvarez, José Coca. "Sunflower oil	1%

miscella degumming with polyethersulfone membranes", Journal of Food Engineering, 2006
Publication

---

5 Tutuk Djoko Kusworo, Danny Soetrisnanto, Nita Aryanti, Dani Puji Utomo et al. "Evaluation of Integrated modified nanohybrid polyethersulfone-ZnO membrane with single stage and double stage system for produced water treatment into clean water", Journal of Water Process Engineering, 2018 — 1%
Publication

---

6 María-José Corbatón-Báguena, Annarosa Gugliuzza, Alfredo Cassano, Rosalinda Mazzei, Lidietta Giorno. "Destabilization and removal of immobilized enzymes adsorbed onto polyethersulfone ultrafiltration membranes by salt solutions", Journal of Membrane Science, 2015 — <1%
Publication

---

7 Leticia R. Firmán, Cecilia Pagliero, Nelio A. Ochoa, José Marchese. "PVDF/PMMA membranes for lemon juice clarification: fouling analysis", Desalination and Water Treatment, 2014 — <1%
Publication

---

8 Emmanouil Tzimtzimis. "Outcome of — <1%

Electrosurgery Versus Scalpel Blade for Intestinal Incisions in Dogs", Veterinary Evidence, 2019
Publication

---

9 Iman Noshadi, Abdolhamid Salahi, Mahmood Hemmati, Fatemeh Rekabdar, Toraj Mohammadi. "Experimental and ANFIS modeling for fouling analysis of oily wastewater treatment using ultrafiltration", Asia-Pacific Journal of Chemical Engineering, 2013 <1%
Publication

---

10 Huiqin ZHANG, Zhaoxiang ZHONG, Weixing LI, Weihong XING, Wanqin JIN. "River Water Purification via a Coagulation-Porous Ceramic Membrane Hybrid Process", Chinese Journal of Chemical Engineering, 2014 <1%
Publication

---

11 Ng, Ching Yin, Abdul Wahab Mohammad, Law Yong Ng, and Jamaliah Md. Jahim. "Membrane fouling mechanisms during ultrafiltration of skimmed coconut milk", Journal of Food Engineering, 2014. <1%
Publication

---

12 Leticia R. Firman, Nelio A. Ochoa, José Marchese, Cecilia L. Pagliero. "Deacidification and solvent recovery of soybean oil by nanofiltration membranes", Journal of <1%

Membrane Science, 2013
Publication

---

13 Jorge Garcia-Ivars, Lucia Martella, Manuele Massella, Carlos Carbonell-Alcaina et al. "Nanofiltration as tertiary treatment method for removing trace pharmaceutically active compounds in wastewater from wastewater treatment plants", Water Research, 2017 <1%
Publication

---

14 S. L. Abidi. "Tocol-derived minor constituents in selected plant seed oils", Journal of the American Oil Chemists Society, 04/2003 <1%
Publication

---

15 Cassano, A.. "Integrated membrane process for the production of highly nutritional kiwifruit juice", Desalination, 20060301 <1%
Publication

---

16 Salahi, A.. "Permeate flux decline during UF of oily wastewater: Experimental and modeling", Desalination, 201002 <1%
Publication

---

17 Hasan, A., C. R. Peluso, T. S. Hull, J. Fieschko, and S. G. Chatterjee. "A surface-renewal model of cross-flow microfiltration", Brazilian Journal of Chemical Engineering, 2013. <1%
Publication

Mihály Zakar, Ildikó Kovács, Péter Muhi, Erika

18	Hanczné Lakatos, Gábor Keszthelyi-Szabó, Zsuzsanna László. "The Effect of Advanced Oxidation Pre-Treatment on the Membrane Filtration Parameters of Dairy Wastewater", Hungarian Journal of Industry and Chemistry, 2017 Publication	<1%
19	Palazzolo, D. J., and F. R. McCarthy. "State and Local Government Organizations and the Formation of the Help America Vote Act", Publius The Journal of Federalism, 2005. Publication	<1%
20	Juan José Torres, Natalia Evelin Rodriguez, Javier Toledo Arana, Nelio Ariel Ochoa, José Marchese, Cecilia Pagliero. "Ultrafiltration polymeric membranes for the purification of biodiesel from ethanol", Journal of Cleaner Production, 2017 Publication	<1%

Exclude quotes	Off	Exclude matches	Off
Exclude bibliography	Off		